

# A New Cell Association Scheme In Heterogeneous Networks

Bin Yang\*, Guoqiang Mao<sup>§</sup>, Xiaohu Ge\*, Tao Han\*

\* School of Electronic Information & Communications, Huazhong University of Science & Technology, Wuhan, China

<sup>§</sup> School of Computing and Communication, University of Technology Sydney, Australia

Corresponding Author: Xiaohu Ge, Email: xhge@mail.hust.edu.cn

**Abstract**—Cell association scheme determines which base station (BS) and mobile user (MU) should be associated with and also plays a significant role in determining the average data rate a MU can achieve in heterogeneous networks. However, the explosion of digital devices and the scarcity of spectra collectively force us to carefully re-design cell association scheme which was kind of taken for granted before. To address this, we develop a new cell association scheme in heterogeneous networks based on joint consideration of the signal-to-interference-plus-noise ratio (SINR) which a MU experiences and the traffic load of candidate BSs<sup>1</sup>. MUs and BSs in each tier are modeled as several independent Poisson point processes (PPPs) and all channels experience independently and identically distributed (*i.i.d.*) Rayleigh fading. Data rate ratio and traffic load ratio distributions are derived to obtain the tier association probability and the average ergodic MU data rate. Through numerical results, We find that our proposed cell association scheme outperforms cell range expansion (CRE) association scheme. Moreover, results indicate that allocating small sized and high-density BSs will improve spectral efficiency if using our proposed cell association scheme in heterogeneous networks.

**Index Terms**—Heterogeneous networks; cell association scheme; traffic load; Poisson point processes

## I. INTRODUCTION

Driven by a new revolution of digital devices like smart phones, tablets and so on, there has been experiencing a tremendous growth of mobile internet traffic in recent years. Traditional network expansion techniques like cell splitting are often utilized by telecom operators to achieve the expected throughput, which are less efficient and proven not to keep up with the pace of traffic proliferation in the near future. Heterogeneous networks then become a promising and attractive network architecture to settle this. Heterogeneous networks are a broad term that refers to the coexistence of different networks (e.g., traditional macrocell and small-cell networks like femtocells and picocells), each of them constituting a network tier. Due to differences in deployment, base stations (BSs) in different tiers may have or use different transmission power levels, radio access technologies, fading environments and spatial densities. Heterogeneous networks are envisioned to cope with most problems of existing network architectures like dead spots, inter-cell interference, less efficient, etc and has been introduced in the LTE-Advanced standardization [1]. Massive

work has been done in heterogeneous networks scenario mainly related with coverage modeling [2], [3], cooperative communications [4], energy consumption modeling [5], [6], interference cancellation [7], interference management [8] and resource allocation [9]–[11], however none of which pays enough attention to existing problems on cell association schemes.

### A. Motivation and related work

In heterogeneous cellular networks, there are more BSs which a MU can choose to be associated with than in traditional homogeneous single-tier cellular networks. Therefore, cell association scheme is an indispensable factor in wireless networks modeling. By using the maximum received signal strength (RSS) as cell association scheme, ElSawy and Hossain quantified the performance gain in the outage probability obtained by introducing cognition into femtocells in two-tier heterogeneous networks [2]. In [12], Ali and Saquib developed a practical yet tractable method of evaluating vertical handover algorithms in a WLAN/Cellular two-tier heterogeneous network and the cell association is also based on the maximum RSS. Dhillon *et al.* [3] proposed a tractable and accurate model for a downlink heterogeneous cellular network consisting of  $K$  tiers of randomly located BSs. Novlan *et al.* aimed to evaluate two fractional frequency reuse (FFR) methods – strict FFR and soft frequency reuse by using Poisson point processes (PPPs) in [13]. The cell association scheme utilized by Dhillon and Novlan is based on the maximum downlink signal-to-interference-plus-noise ratio (SINR). Also, the nearest BS cell association scheme is applied in some literatures like [5], [14]. Yong Sheng *et al.* investigated the design and the associated tradeoffs of energy efficient heterogeneous cellular networks through the deployment of sleeping strategies in [5]. In [14], Mukherjee provided a general theoretical analysis of the distribution of the SINR at an arbitrarily-located MU in heterogeneous networks.

From above literatures, existing cell association schemes have been mainly based on the RSS, SINR or the distance from nearby BSs to determine which BS and MU should be connected with each other. This is legitimate for traditional homogeneous single-tier cellular networks where the RSS or the SINR serves as a good indicator of the data rate received by the MU. However, it is no longer the case in heterogeneous networks in which BSs from different tiers transmit wireless signals at very different power levels,

<sup>1</sup>Candidate BSs is comprehended as the set of BSs which a mobile user (MU) is most likely associated with.

varying from milliWatt (mW) to Watt (W): **a)** the higher RSS may be a result of the higher transmission power used by the BS. It may cause congestions in BSs which have higher RSS and idleness in BSs whose RSS is lower whereas can still guarantee successful transmission. This result brings unbalance and inequity among BSs in different tier networks; **b)** the number of MUs served by a small-cell BS is typically small due to its much smaller coverage. Consequently, the current traffic load of the BS plays a significant role in determining the share of BS capacity received by each MU. For example, the joining of a MU into a small-cell BS currently serving one MU may halve the data rate received by the current MU; **c)** as for choosing the nearest BS for association, it is so impractical that only used for theoretical analysis. Thus, it is no longer optimum to determine cell association solely based on the RSS, the SINR or the distance from nearby BSs.

As described above, cell association schemes play an important role in determining the allocation of spectral resource in BSs, the transmission rate that a MU can achieve and even the energy consumption of MUs. In [15], [16], a solution was proposed to partially solve the problem **a)** by introducing a biased factor  $\Omega$  or  $B$  into the RSS, which allows an expansion of the coverage of small-cell BSs. The effectiveness of the scheme however remains questionable in networks with inhomogeneous user density, e.g. MUs clustering around BSs. In [17], authors mentioned the problem **b)** in the subsection of resource allocation. However, per MU data rate is only a performance metric with the form of rate coverage and the used cell association scheme was still conventional, which left these problems unsolved.

### B. Contributions and organization

To solve problems **a)**, **b)** and **c)**, a spectrum efficient cell association scheme based on the joint consideration of the received SINR and the traffic load of BSs is proposed for heterogeneous networks. To match real BSs deployment scenarios, PPP is used to model heterogeneous cellular networks in this article, which has been strengthened by the empirical validation [18] and the theoretical validation [19]. The contributions and novelties of this paper are summarized as follows.

- 1) A new cell association scheme is proposed with two steps for heterogeneous networks. The first step is mainly for choosing the candidate BSs by traditional method, i.e., the nearest  $n$  BSs, while the second step determines the ultimate one BS based on the consideration of the received SINR experienced by a MU and the traffic load of candidate BSs.
- 2) Following the cell association scheme and taking a three-tier heterogeneous network as an example, the tier association probability and the average ergodic MU data rate are derived for numerical analysis.
- 3) Based on numerical results, the new cell association scheme outperforms CRE association scheme.

The remainder of this paper is organized as follows. In section II, we present our network model and propose a

new cell association scheme in general case. A three-tier heterogeneous network is analyzed in section III. Moreover, the tier association probability of heterogeneous networks is derived for performance analysis. Section IV presents the numerical results of the proposed cell association scheme. Section V concludes this paper.

## II. NETWORK MODEL AND PROPOSED CELL ASSOCIATION SCHEME

We Consider a  $K$ -tier heterogeneous downlink cellular network which consists of macrocells, picocells, femtocells, etc. BSs of each tier are assumed to be spatially distributed following independent homogenous PPPs denoted by  $\Phi_k$ ,  $k \in \{1, 2, \dots, K\}$ . The BS intensity of the  $k$ -th tier network is  $\lambda_k$ ,  $k \in \{1, 2, \dots, K\}$ . MUs are located according to a homogeneous point process denoted by  $\Phi_u$  with intensity  $\lambda_u$ . All BSs in the same tier network are configured with the same transmission power  $P_k$ ,  $k \in \{1, 2, \dots, K\}$  and share the same bandwidth. BSs in different tier networks are configured with different bandwidths. Moreover, within a cell, MSs are allocated by orthogonal frequencies. Therefore, there is no intra-cell interference in a cell. Also for simplicity, the open access policy is applied for MUs. It means all MUs can be served by BSs in any tier networks.

We propose a new cell association scheme that bases its cell association decision on the instant traffic load of each BS and the transmission rate that can be allocated by the BS. More specifically, the cell association scheme can be divided into two steps.

- 1) If a MU wants to be associated with a BS, it will firstly choose  $n$  nearest BSs from each tier as the candidate BSs. The candidate BS set is defined as  $\Omega_B = \{(k, i) | k \in \{1, 2, \dots, K\}, i \in [1, n]\}$ , where  $k$  is the  $k$ -th tier network in a heterogeneous network and  $i$  is the  $i$ -th BS in the  $n$  nearest BSs from the  $k$ -th tier network. For example,  $(1, 3)$  represents the 3rd BS in the 1st tier network. The total number of BSs in  $\Omega_B$  is  $nK$ .
- 2) The MU will select a candidate BS from  $\Omega_B$ . This selected BS will send data to the MU with the maximum average transmission rate, i.e.,  $\frac{B_{k,i}}{N_{k,i}+1} \cdot \ln(1 + \text{SINR}_{k,i})$ , where  $B_{k,i}$  and  $N_{k,i}$  are the total bandwidth of a candidate BS in set  $\Omega_B$  and the instant BS traffic load, respectively.  $\text{SINR}_{k,i}$  is the MU instant SINR associated with a BS  $(k, i)$  in the set  $\Omega_B$ . It is assumed that the total BS bandwidth is shared equally among all associated MUs.<sup>2</sup>

## III. PERFORMANCE ANALYSIS

Without generality, in the following we will analyse the scenario when  $K = 3$  and  $n = 1$ . The network being considered is a three-tier heterogeneous network and only the nearest BS at each tier from a MU can be chosen as candidate BSs. The analysed three-tier heterogeneous network is depicted in Fig. 1.

<sup>2</sup>In our following analysis, the candidate BS  $(k, i)$  can be denoted by  $k$  when  $n = 1$ . However, we'll keep using  $(k, i)$  for completeness and preciseness.

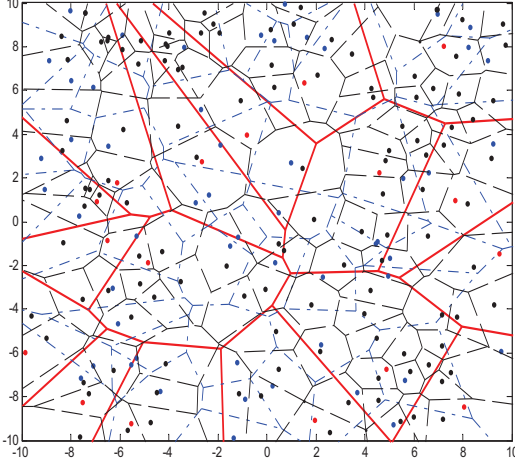


Figure 1. The three-tier heterogeneous network ( $20\text{km} \times 20\text{km}$ ) modeled as a superposition of three independent Poisson Voronoi tessellations. These polygons are 1st tier cells (edges with red solid lines), 2nd tier cells (edges with blue dot-dash lines) and 3rd tier cells (edges with black dotted lines).

#### A. The downlink SINR distribution

For downlink transmission of a BS ( $k, i$ ) to a MU which is located at the origin  $o$ , the SINR experienced by this MU is expressed by

$$\text{SINR}_{k,i} = \frac{P_k h_{k,i} r_{k,i}^{-\alpha}}{\sum_{m \in \Omega'_k} P_k h_{k,m} r_{k,m}^{-\alpha} + \sigma^2}, \quad (1)$$

where  $\Omega'_k$  is set of interferers in the  $k$ -th tier network.  $h_{k,i}$  and  $h_{k,m}$  are channel power gains due to small-scale fading between the considered MU and BS ( $k, i$ ), ( $k, m$ ), respectively. For convenience and without generality, we assume  $h_{k,i} \sim \exp(1)$  and  $h_{k,m} \sim \exp(1)$ . The background noise is assumed to be additive white Gaussian with variance  $\sigma^2$ .  $r_{k,i}^{-\alpha}$  and  $r_{k,m}^{-\alpha}$  are path losses with  $\alpha$  being the path loss exponent,  $r_{k,i}$  and  $r_{k,m}$  being the respective Euclidean distance to the corresponding BS ( $k, i$ ) and ( $k, m$ ), respectively.

Referring to [5], the coverage probability that a MU is covered by its nearest BS in a particular tier  $k$  is derived as follows

$$\begin{aligned} P_c^k(x) &= \Pr(\text{SINR}_{k,i} > x) \\ &= 2\pi\lambda_k \int_{r=0}^{+\infty} r \exp[-\pi r^2 \lambda_k (1 + \varphi(x))] \times \\ &\quad \exp\left(-\frac{r^\alpha x \sigma^2}{P_k}\right) dr, \end{aligned} \quad (2)$$

where  $\varphi(x) = x^{\frac{2}{\alpha}} \int_{x^{-\frac{2}{\alpha}}}^{+\infty} \frac{1}{1+y^{\frac{\alpha}{2}}} dy$ .  $P_c^k(x)$  is the complementary cumulative distribution function (CCDF) of  $\text{SINR}_{k,i}$  and the cumulative distribution function (CDF) of  $\text{SINR}_{k,i}$  is  $1 - P_c^k(x)$ . By taking a derivative of the CDF of  $\text{SINR}_{k,i}$  with respect to  $x$ , the probability density function (PDF) of  $\text{SINR}_{k,i}$  is obtained by

$$\begin{aligned} f_{\text{SINR}_{k,i}}(x) &= 2\pi\lambda_k \int_{r=0}^{+\infty} r \left[ \pi r^2 \lambda_k \varphi'(x) + \frac{r^\alpha \sigma^2}{P_k} \right] \times \\ &\quad \exp[-\pi r^2 \lambda_k (1 + \varphi(x))] \times \\ &\quad \exp\left(-\frac{r^\alpha x \sigma^2}{P_k}\right) dr \end{aligned} \quad (3)$$

with

$$\varphi'(x) = \frac{2}{\alpha} \left[ \frac{\varphi(x)}{x} + \frac{1}{1+x} \right]. \quad (4)$$

#### B. The tier association probability

The spatial average data rate a MU can achieve is denoted by  $\overline{C}_k$ ,  $k \in \{1, 2, 3\}$  and the event that the considered MU is associated with a BS in the  $k$ -th tier network is denoted by ( $N_{\text{Tier}} = k$ ). We'll apply Slivnyak's theorem to the following analysis on a MU that located at the origin  $o$ , which implies that conditioning on having that user at the origin, properties of all coexisting PPPs maintaining the same. Using the above association scheme in section II, the probability that a MU is associated with the 1st tier BS (1,  $i$ ) is

$$\begin{aligned} \mathcal{T}_1 &= \Pr(N_{\text{Tier}} = 1) \\ &= \Pr\left(\overline{C}_1 > \max_{j \neq 1} \overline{C}_j\right) \\ &= \Pr\left[\frac{B_{1,i}}{N_{1,i+1}} \ln(1 + \text{SINR}_{1,i}) > \frac{B_{2,i}}{N_{2,i+1}} \ln(1 + \text{SINR}_{2,i}), \frac{B_{1,i}}{N_{1,i+1}} \ln(1 + \text{SINR}_{1,i}) > \frac{B_{3,i}}{N_{3,i+1}} \ln(1 + \text{SINR}_{3,i})\right] \\ &\stackrel{\text{(I)}}{=} \prod_{j=2}^3 \Pr\left[\frac{B_{1,i}}{N_{1,i+1}} \ln(1 + \text{SINR}_{1,i}) > \frac{B_{j,i}}{N_{j,i+1}} \ln(1 + \text{SINR}_{j,i})\right] \\ &= \prod_{j=2}^3 \Pr\left[\frac{N_{1,i+1}}{N_{j,i+1}} < \frac{B_{1,i}}{B_{j,i}} \cdot \frac{\ln(1 + \text{SINR}_{1,i})}{\ln(1 + \text{SINR}_{j,i})}\right] \\ &\stackrel{\text{(II)}}{=} \prod_{j=2}^3 \Pr\left[N_{1/j} < \frac{B_{1,i}}{B_{j,i}} \cdot \text{SINR}_{1/j}\right] \\ &\stackrel{\text{(III)}}{=} \prod_{j=2}^3 \int_0^{+\infty} F_{N_{1/j}}\left(\frac{B_{1,i}}{B_{j,i}} \cdot x\right) \cdot f_{\text{SINR}_{1/j}}(x) dx \end{aligned} \quad (5)$$

where (I) is due to the independence between two events  $\{\overline{C}_1 > \overline{C}_2\}$  and  $\{\overline{C}_1 > \overline{C}_3\}$ ; in (II),  $N_{1/j}$ ,  $\text{SINR}_{1/j}$  denote  $\frac{N_{1,i+1}}{N_{j,i+1}}$  and  $\frac{\ln(1 + \text{SINR}_{1,i})}{\ln(1 + \text{SINR}_{j,i})}$ , respectively; (III) is obtained by applying the law of total probability where  $F_{N_{1/j}}(x)$  is the CDF of  $\frac{N_{1,i+1}}{N_{j,i+1}}$  and  $f_{\text{SINR}_{1/j}}(x)$  denotes the PDF of  $\frac{\ln(1 + \text{SINR}_{1,i})}{\ln(1 + \text{SINR}_{j,i})}$ .

1) *The CDF of  $\frac{N_{1,i+1}}{N_{j,i+1}}$* : In this paper, it is assumed that each BS has a unique saturated downlink transmission queue for each MU. This assumption implies that MU always has data to receive from a BS which covers and associates that MU<sup>3</sup>. Each MU choose the associating BS with probabilities denoted by  $\mathcal{T}_k$ ,  $k \in \{1, 2, 3\}$ . Thus, three point processes denoted by  $\Phi_u^1$ ,  $\Phi_u^2$  and  $\Phi_u^3$  are formed by thinning the original PPP  $\Phi_u$ . The thinned processes are the locations of MUs which are associated with the 1st, the 2nd and the

<sup>3</sup>The shape of a BS's coverage is Voronoi-tessellated.

3rd tier BSs. The thinned point processes are still PPPs and intensities are  $\mathcal{T}_1\lambda_u$ ,  $\mathcal{T}_2\lambda_u$  and  $\mathcal{T}_3\lambda_u$ , respectively.

Through interpretations above, the probability mass function (PMF) of  $N_{k,i}$ <sup>4</sup> is given by

$$\begin{aligned}
f_{N_{k,i}}(n) &= \Pr(N_{k,i} = n) \\
&= \int_0^{+\infty} \frac{(\mathcal{T}_k\lambda_u s)^n e^{-\mathcal{T}_k\lambda_u s}}{n!} \cdot f_{S_k}(s) ds \\
&= \int_0^{+\infty} \frac{(\mathcal{T}_k\lambda_u s)^n e^{-\mathcal{T}_k\lambda_u s}}{n!} \cdot \frac{(c\lambda_k)^c s^{c-1} e^{-c\lambda_k s}}{\Gamma(c)} ds \\
&= \frac{(\mathcal{T}_k\lambda_u)^n}{n!} \cdot \frac{(c\lambda_k)^c}{\Gamma(c)} \times \\
&\int_0^{+\infty} \frac{(\mathcal{T}_k\lambda_u s)^n e^{-\mathcal{T}_k\lambda_u s}}{n!} s^{n+c-1} e^{-s(\mathcal{T}_k\lambda_u + c\lambda_k)} ds, \\
&= \frac{(\mathcal{T}_k\lambda_u)^n (c\lambda_k)^c}{n! \Gamma(c)} \cdot \frac{\Gamma(n+c)}{(\mathcal{T}_k\lambda_u + c\lambda_k)^{n+c}} \times \\
&\int_0^{+\infty} \frac{(\mathcal{T}_k\lambda_u + c\lambda_k)^{n+c}}{\Gamma(n+c)} \cdot s^{n+c-1} \cdot e^{-s(\mathcal{T}_k\lambda_u + c\lambda_k)} ds \\
&\stackrel{(I)}{=} \frac{(\mathcal{T}_k\lambda_u)^n (c\lambda_k)^c}{(\mathcal{T}_k\lambda_u + c\lambda_k)^{n+c}} \cdot \frac{\Gamma(n+c)}{\Gamma(n+1)\Gamma(c)}
\end{aligned} \tag{6}$$

where  $\Gamma(\cdot)$  is the Gamma function;  $f_{S_k}(s) \approx \frac{(c\lambda_k)^c s^{c-1} e^{-c\lambda_k s}}{\Gamma(c)}$  is the PDF of the Voronoi cell area of the  $k$ -th tier network obtained through simulations and  $c = 3.575$  is a constant [20]. (I) is obtained due to the integration of the formula with underline is 1 over the domain. Actually, the format of the formula with underline is the PDF of Gamma distribution like  $y = \frac{x^{k-1} e^{-x/\theta}}{\theta^k \Gamma(k)}$ .

The CDF of  $\frac{N_{1,i}+1}{N_{j,i}+1}$  is derived by

$$\begin{aligned}
F_{N_{1/j}}(x) &= \Pr\left(\frac{N_{1,i}+1}{N_{j,i}+1} < x\right) \\
&= \Pr[N_{1,i} < (N_{j,i} + 1)x - 1] \\
&\stackrel{(I)}{=} \sum_{t=0}^{\infty} \Pr[N_{1,i} < (t+1)x - 1 \mid N_{j,i} = t] \times \\
&\quad \Pr(N_{j,i} = t) \\
&= \sum_{t=0}^{\infty} F_{N_{1,i}}[\lfloor (t+1)x - 1 \rfloor] \cdot f_{N_{j,i}}(t)
\end{aligned} \tag{7}$$

where  $F_{N_{k,i}}(l)$  is the CDF of  $N_{k,i}$  which is derived by

$$\begin{aligned}
F_{N_{k,i}}(l) &= \sum_{n=0}^l f_{N_{k,i}}(n) \\
&= \sum_{n=0}^l \frac{(\mathcal{T}_k\lambda_u)^n (c\lambda_k)^c}{(\mathcal{T}_k\lambda_u + c\lambda_k)^{n+c}} \cdot \frac{\Gamma(n+c)}{\Gamma(n+1)\Gamma(c)}, \quad l \in [0, \infty)
\end{aligned} \tag{8}$$

$\lfloor \cdot \rfloor$  is the floor function and (I) follows the law of total probability. Substituting (8) back in (7), we obtain the CDF of  $\frac{N_{1,i}+1}{N_{j,i}+1}$  as follows

$$\begin{aligned}
F_{N_{1/j}}(x) &= \sum_{t=0}^{\infty} \left\{ \frac{(\mathcal{T}_j\lambda_u)^t (c\lambda_j)^c}{(\mathcal{T}_j\lambda_u + c\lambda_j)^{t+c}} \cdot \frac{\Gamma(t+c)}{\Gamma(t+1)\Gamma(c)} \times \right. \\
&\quad \left. \sum_{n=0}^{\lfloor (t+1)x - 1 \rfloor} \frac{(\mathcal{T}_1\lambda_u)^n (c\lambda_1)^c}{(\mathcal{T}_1\lambda_u + c\lambda_1)^{n+c}} \cdot \frac{\Gamma(n+c)}{\Gamma(n+1)\Gamma(c)} \right\}
\end{aligned} \tag{9}$$

<sup>4</sup> in this paper, traffic load of a BS is defined as the total number of MUs associated with that BS.

2) *The PDF of  $\frac{\ln(1+\text{SINR}_{1,i})}{\ln(1+\text{SINR}_{j,i})}$* : Let the PDF of  $\text{SINR}_{k,i}$  be  $f_{\text{SINR}_{k,i}}(x)$  and the CDF be  $F_{\text{SINR}_{k,i}}(x)$ , then the CDF of  $\ln(1 + \text{SINR}_{k,i})$  is derived by

$$\begin{aligned}
F_{\ln(1+\text{SINR}_{k,i})}(y) &= \Pr[\ln(1 + \text{SINR}_{k,i}) < y] \\
&= \Pr(\text{SINR}_{k,i} < e^y - 1) \\
&= F_{\text{SINR}_{k,i}}(e^y - 1)
\end{aligned} \tag{10}$$

By taking a derivative with respect to  $y$  in both sides of (10), the PDF of  $\ln(1 + \text{SINR}_{k,i})$  is obtained by

$$f_{\ln(1+\text{SINR}_{k,i})}(y) = e^y \cdot f_{\text{SINR}_{k,i}}(e^y - 1). \tag{11}$$

Let  $f_{j_o}(x, y)$  denote the joint probability density function (JPDF) of random variable tuple  $(\ln(1 + \text{SINR}_{1,i}), \ln(1 + \text{SINR}_{j,i}))$ ,  $j \in \{2, 3\}$ . The PDF of  $\frac{\ln(1+\text{SINR}_{1,i})}{\ln(1+\text{SINR}_{j,i})}$  is derived by

$$\begin{aligned}
f_{\text{SINR}_{1/j}}(z) &= \int_{-\infty}^{\infty} |y| \cdot f_{j_o}(zy, y) dy \\
&\stackrel{(I)}{=} \int_0^{\infty} y \cdot f_{j_o}(zy, y) dy
\end{aligned} \tag{12}$$

where (I) is obtained by using the ratio distribution (or quotient distribution) formula of two nonnegative random variables. Because of the independence of the two variables, i.e.,  $\ln(1 + \text{SINR}_{1,i})$  and  $\ln(1 + \text{SINR}_{j,i})$ ,  $f_{j_o}(x, y)$  is expressed by

$$\begin{aligned}
f_{j_o}(x, y) &= f_{\ln(1+\text{SINR}_{1,i})}(x) \cdot f_{\ln(1+\text{SINR}_{j,i})}(y) \\
&= e^{x+y} f_{\text{SINR}_{1,i}}(e^x - 1) \cdot f_{\text{SINR}_{j,i}}(e^y - 1)
\end{aligned} \tag{13}$$

Substituting (13) back into (12), we obtain the PDF of  $\frac{\ln(1+\text{SINR}_{1,i})}{\ln(1+\text{SINR}_{j,i})}$  as follows

$$f_{\text{SINR}_{1/j}}(z) = \int_0^{\infty} y e^{(z+1)y} f_{\text{SINR}_{1,i}}(e^{zy} - 1) \times f_{\text{SINR}_{j,i}}(e^y - 1) dy, \tag{14}$$

where  $f_{\text{SINR}_{k,i}}(x)$  is given by (3).

Similarly, by repeating the derivations above, the probabilities that a MU is associated with a BS in the 2nd and the 3rd tier network are obtained, i.e.,

$$\mathcal{T}_2 = \prod_{j=1, j \neq 2}^3 \int_0^{+\infty} F_{N_{2/j}}\left(\frac{B_{2,i}}{B_{j,i}} \cdot x\right) \cdot f_{\text{SINR}_{2/j}}(x) dx, \tag{15}$$

$$\mathcal{T}_3 = \prod_{j=1}^2 \int_0^{+\infty} F_{N_{3/j}}\left(\frac{B_{3,i}}{B_{j,i}} \cdot x\right) \cdot f_{\text{SINR}_{3/j}}(x) dx. \tag{16}$$

Using numerical method, the exact value of  $\mathcal{T}_k$ ,  $k \in \{1, 2, 3\}$  are obtained by solving equations (5), (15) and (16).

### C. The average ergodic MU data rate

In this subsection, we focus on the average ergodic MU data rate of a MU in a K-tier heterogeneous network. We assume that Shannon's capacity can be achieved by some coding methods. The average ergodic MU data rate can be obtained by considering per tier user data rates weighted by the corresponding tier association probabilities. The average ergodic MU rate in a 3-tier heterogeneous network is given by

$$\bar{\mathfrak{R}} = \sum_{k=1}^3 \mathcal{T}_k \mathfrak{R}_k. \tag{17}$$

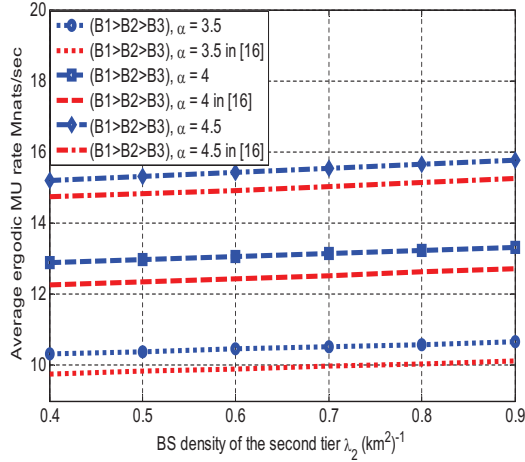


Figure 2. The average ergodic MU data rate with respect to the density of the 2nd tier BSs with spectral allocation of (B1>B2>B3) in a three-tier heterogeneous network.

$\mathfrak{R}_k$  is the ergodic MU data rate conditioning on a MU is associated with a specific BS in the  $k$ -th tier network which is given by

$$\begin{aligned} \mathfrak{R}_k &= \mathbf{E} [B_{k,i} \cdot \ln(1 + \text{SINR}_{k,i})] \\ &\stackrel{(1)}{=} B_{k,i} \int_0^\infty \Pr[\ln(1 + \text{SINR}_{k,i}) > t] dt, \quad (18) \\ &= B_{k,i} \int_0^\infty P_c^k(e^t - 1) dt \end{aligned}$$

where (1) is derived because  $\ln(1 + \text{SINR}_{k,i})$  is a nonnegative random variable;  $\mathbf{E}(\cdot)$  is an expectation operator and  $P_c^k(\cdot)$  is given by (2). Substituting (18) into (17), we can get the unconditional average ergodic MU data rate as follows

$$\begin{aligned} \bar{\mathfrak{R}} &= \sum_{k=1}^3 2\pi\lambda_k \mathcal{T}_k B_{k,i} \int_0^\infty \int_{r=0}^{+\infty} r \times \\ &\quad \exp[-\pi r^2 \lambda_k (1 + \varphi(e^t - 1))] \times \cdot \quad (19) \\ &\quad \exp\left(-\frac{r^\alpha \sigma^2 (e^t - 1)}{P_k}\right) dr dt \end{aligned}$$

#### IV. NUMERICAL RESULTS AND DISCUSSIONS

This section presents numerical results of previous sections, followed by discussions. Parameters used in this article are referred to existing work focused on heterogeneous networks. Specifically, we assume that  $\sigma^2 = 0$  which denotes a interference-limited scenario. BS densities and BS transmission powers are  $\lambda_2 = 2\lambda_1$ ,  $\lambda_3 = 20\lambda_1$ ,  $\lambda_u = 50\lambda_1$ ,  $P_1 = 53\text{dBm}$ ,  $P_2 = 33\text{dBm}$ ,  $P_3 = 23\text{dBm}$  [15], [17]. Allocations of spectra are divided into 4 cases, i.e., **(B1>B2>B3)**:  $B_1 = 15\text{MHz}$ ,  $B_2 = 10\text{MHz}$ ,  $B_3 = 5\text{MHz}$ ; **(B1>B3>B2)**:  $B_1 = 15\text{MHz}$ ,  $B_2 = 5\text{MHz}$ ,  $B_3 = 10\text{MHz}$ ; **(B2>B3>B1)**:  $B_1 = 5\text{MHz}$ ,  $B_2 = 15\text{MHz}$ ,  $B_3 = 10\text{MHz}$ ; and **(B3>B2>B1)**:  $B_1 = 5\text{MHz}$ ,  $B_2 = 10\text{MHz}$ ,  $B_3 = 15\text{MHz}$  [17].<sup>5</sup> In the following, we will use default values above unless otherwise declared.

Fig. 2 shows the average ergodic MU data rate with respect to the density of the 2nd tier BSs  $\lambda_2$  which varies from  $0.4(\text{km}^2)^{-1}$  to  $0.9(\text{km}^2)^{-1}$  considering three different path loss exponents  $\alpha$ . We find that the average ergodic

<sup>5</sup>There are 6 cases of the allocations of spectra in three-tier heterogeneous networks in total. However, we only analyze 4 typical cases therein.

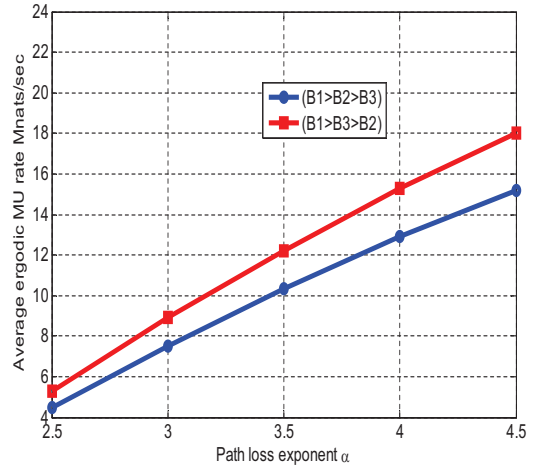


Figure 3. The average ergodic MU data rate with respect to path loss exponent with two kinds of spectral allocations in a three-tier heterogeneous network.

MU rate increases slowly with the increasing BS density when we fix the path loss exponent. Also, our proposed cell association scheme outperforms the CRE association scheme analyzed in [15], which indicates the effectiveness of ours'. Path loss exponent has more effects on the average ergodic MU data rate when the BS density is fixed. Higher path loss exponent always results in higher average ergodic MU data rate.

Fig. 3 compares the average ergodic MU data rate with respect to path loss exponent with two kinds of spectral allocations, i.e., (B1>B2>B3) and (B1>B3>B2). The average ergodic MU data rate increases with the increasing path loss exponent when spectral allocation is fixed, which indicates that to some degree higher path loss exponent contributes network performance. When path loss exponent is fixed, (B1>B3>B2) performs better than (B1>B2>B3). (B1>B2>B3) represents traditional spectral allocation which distributes more spectral resource towards towered BSs, while in (B1>B3>B2) small BSs have more spectral resource than towered BSs. It is implied that if using our proposed cell association scheme, small sized and high-density BSs should be allocated more spectral resource to obtain better holistic performance.

Fig. 4 and fig. 5 illustrate the average ergodic MU data rate with respect to path loss exponent with two kinds of spectral allocations. We obtain similar conclusions obtained from fig. 3. However, the gap between the two curves of (B1>B2>B3) and (B2>B3>B1) in fig. 4 and the gap between the two curves of (B1>B2>B3) and (B3>B2>B1) in fig. 5 are bigger than that in fig. 3, which again indicates that small sized and high-density BSs should be allocated more spectral resource if using our proposed cell association scheme.

#### V. CONCLUSIONS

In this paper, motivated by the problems of existing cell association schemes which are merely based on one indicator like RSS, SINR or distance from nearby BSs, we propose a new cell association scheme by joint consideration of

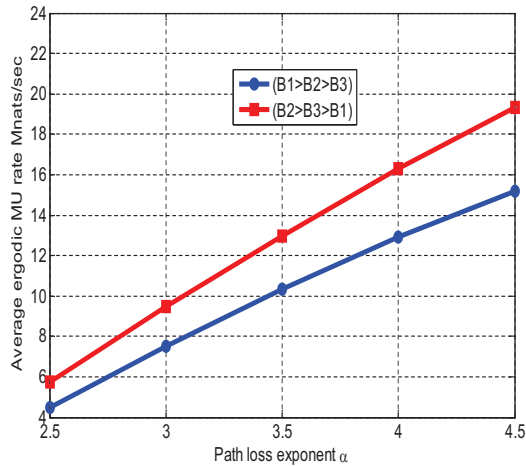


Figure 4. The average ergodic MU rate with respect to path loss exponent with two kinds of spectral allocations in a three-tier heterogeneous network.

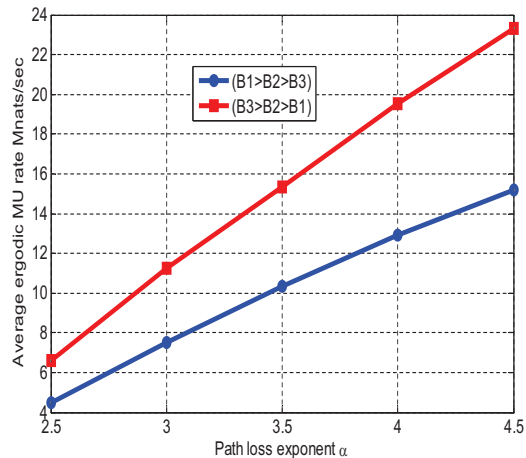


Figure 5. The average ergodic MU rate with respect to path loss exponent with two kinds of spectral allocations in a three-tier heterogeneous network.

SINR and traffic load in heterogeneous networks. Through numerical results, we find that our proposed cell association scheme outperforms CRE association scheme. Also, the results provide some insights of spectral allocation by using our proposed cell association scheme, which implies that allocating small sized and high-density BSs more spectral resource results in better holistic performance.

Still, some work need to be done to further this proposed cell association scheme. For instance, if the number of candidate BSs  $n$  in each tier network is more than one, the corresponding analysis may be more general. And also, adding shadowing may make the scenario more realistic.

#### ACKNOWLEDGMENT

The authors would like to acknowledge the support from the International Science and Technology Cooperation Program of China (Grant No. 2014DFA11640 and 2012DFG12250), the National Natural Science Foundation of China (NSFC) (Grant No. 61271224, 61471180 and 61301128), NFSC Major International Joint Research

Project (Grant No. 61210002), the Hubei Provincial Science and Technology Department (Grant No. 2013BHE005), the Fundamental Research Funds for the Central Universities (Grant 2013QN136, 2014QN155 and 2013ZZGH009), and EU FP7-PEOPLE-IRSES (Contract/Grant No. 247083, 318992 and 610524).

#### REFERENCES

- [1] R. Hu and Y. Qian, *Heterogeneous cellular networks*. John Wiley & Sons, 2013.
- [2] H. ElSawy and E. Hossain, "Two-tier hetnets with cognitive femto-cells: Downlink performance modeling and analysis in a multichannel environment," *IEEE Trans. Mobile Comput.*, vol. 13, no. 3, pp. 649–663, 2014.
- [3] H. S. Dhillon, R. K. Ganti, F. Baccelli, and J. G. Andrews, "Modeling and analysis of k-tier downlink heterogeneous cellular networks," *IEEE J. Sel. Areas Commun.*, vol. 30, no. 3, pp. 550–560, 2012.
- [4] Q. Li, R. Hu, Y. Qian, and G. Wu, "Cooperative communications for wireless networks: techniques and applications in lte-advanced systems," *IEEE Wireless Commun.*, vol. 19, no. 2, pp. –, April 2012.
- [5] S. Yong Sheng, T. Q. S. Quek, M. Kountouris, and S. Hyundong, "Energy efficient heterogeneous cellular networks," *IEEE J. Sel. Areas Commun.*, vol. 31, no. 5, pp. 840–850, 2013.
- [6] R. Hu and Y. Qian, "An energy efficient and spectrum efficient wireless heterogeneous network framework for 5g systems," *IEEE Commun. Mag.*, vol. 52, no. 5, pp. 94–101, May 2014.
- [7] L. Jemin, J. G. Andrews, and H. Daesik, "Spectrum-sharing transmission capacity with interference cancellation," *IEEE Trans. Commun.*, vol. 61, no. 1, pp. 76–86, 2013.
- [8] L. Chun-Hung and J. G. Andrews, "Ergodic transmission capacity of wireless ad hoc networks with interference management," *IEEE Trans. Wireless Commun.*, vol. 11, no. 6, pp. 2136–2147, 2012.
- [9] A. R. Elsharif, D. Zhi, L. Xin, and J. Hamalainen, "Resource allocation in two-tier heterogeneous networks through enhanced shadow chasing," *IEEE Trans. Wireless Commun.*, vol. 12, no. 12, pp. 6439–6453, 2013.
- [10] L. Qian, R. Q. Hu, Q. Yi, and W. Geng, "Intracell cooperation and resource allocation in a heterogeneous network with relays," *IEEE Trans. Veh. Technol.*, vol. 62, no. 4, pp. 1770–1784, 2013.
- [11] S. Singh and J. G. Andrews, "Joint resource partitioning and offloading in heterogeneous cellular networks," *IEEE Trans. Wireless Commun.*, vol. 13, no. 2, pp. 888–901, 2014.
- [12] T. Ali and M. Saquib, "Performance evaluation of wlan/cellular media access for mobile voice users under random mobility models," *IEEE Trans. Wireless Commun.*, vol. 10, no. 10, pp. 3241–3255, 2011.
- [13] T. D. Novlan, R. K. Ganti, A. Ghosh, and J. G. Andrews, "Analytical evaluation of fractional frequency reuse for ofdma cellular networks," *IEEE Trans. Wireless Commun.*, vol. 10, no. 12, pp. 4294–4305, 2011.
- [14] S. Mukherjee, "Distribution of downlink sinr in heterogeneous cellular networks," *IEEE J. Sel. Areas Commun.*, vol. 30, no. 3, pp. 575–585, 2012.
- [15] J. Han-Shin, S. Young Jin, X. Ping, and J. G. Andrews, "Heterogeneous cellular networks with flexible cell association: A comprehensive downlink sinr analysis," *IEEE Trans. Wireless Commun.*, vol. 11, no. 10, pp. 3484–3495, 2012.
- [16] C. H. M. de Lima, M. Bennis, and M. Latva-aho, "Statistical analysis of self-organizing networks with biased cell association and interference avoidance," *IEEE Trans. Veh. Technol.*, vol. 62, no. 5, pp. 1950–1961, 2013.
- [17] S. Singh, H. S. Dhillon, and J. G. Andrews, "Offloading in heterogeneous networks: Modeling, analysis, and design insights," *IEEE Trans. Wireless Commun.*, vol. 12, no. 5, pp. 2484–2497, 2013.
- [18] J. G. Andrews, F. Baccelli, and R. K. Ganti, "A tractable approach to coverage and rate in cellular networks," *IEEE Trans. Commun.*, vol. 59, no. 11, pp. 3122–3134, 2011.
- [19] B. Blaszczyszyn, M. K. Karray, and H. P. Keeler, "Using poisson processes to model lattice cellular networks," in *Proc. IEEE INFOCOM 2013*, pp. 773–781.
- [20] J.-S. Ferenc and Z. Néda, "On the size distribution of poisson voronoi cells," *Physica A: Statistical Mechanics and its Applications*, vol. 385, no. 2, pp. 518–526, 2007.